

Quantum control with linear chirp in two-subband n -type doped quantum wells

Adriano A. Batista¹ and D. S. Citrin²¹*Instituto de Física, Universidade de Brasília, Caixa Postal 04455, Brasília, Distrito Federal 70919-970, Brazil*²*School of Electrical and Computer Engineering, Georgia Institute of Technology, Atlanta, Georgia 30332-0250, USA
and Georgia Tech Lorraine, Metz Technopôle, 2-3 rue Marconi, 57070 Metz, France*

(Received 5 July 2006; published 13 November 2006)

We obtain pulse-driven population inversions in two-subband quantum wells (QW's) with a time-varying transition energy. We achieve this by using linearly chirped pulses with the center frequency given by a fit of the time-varying transition energy obtained from the effective nonlinear Bloch equations. The coherent population inversions (Rabi oscillations) are given for square QW's and for dc-biased square QW's. We further verify that the time-dependent polarization of the intersubband transitions can also be controlled.

DOI: [10.1103/PhysRevB.74.195318](https://doi.org/10.1103/PhysRevB.74.195318)

PACS number(s): 78.67.De, 73.43.Lp, 73.63.Hs

I. INTRODUCTION

Two-level quantum systems driven at resonance by electromagnetic pulses give rise to coherent oscillations in the populations known as Rabi oscillations (RO's).¹ When the pulse has a slowly varying envelope its area $\mathcal{A}(t) = \mu \int_{-\infty}^t F_0(s) ds$ gives a measure of the coherent evolution on the Bloch sphere, where μ is the dipole moment and $F_0(s)$ is the pulse envelope. If $\mathcal{A}(\infty)$ is an even multiple of π there is no energy absorption and the pulse propagates without decay in a single-resonance two-level atomic medium—a result known as self-induced transparency.² On the other hand, if the area is an odd multiple of π it causes population inversion and the pulse is rapidly attenuated. This occurs only if the pulse duration is shorter than the homogeneous depopulation and decoherence times T_1 and T_2 and also any dephasing time due to inhomogeneous broadening and detuning. The RO concept provides the basis on which most theory and experiment on coherent optical pulses interacting with two-level atoms is done.^{3,4} The ability to produce RO's in a given system, moreover, indicates whether that system is a candidate for more elaborate coherent manipulation, such as in coherent control experiments or for quantum computing.

Semiconductors, however, provide only an approximate realization of two-level systems. Nevertheless, phenomena closely related to two-level RO's have been observed. It has already been shown experimentally in semiconductors that RO's can occur.^{5,6} More recently in heterostructures, π pulses have been used to perform a single-electron coherent turnstile in quantum dots under a dc bias.⁷ Theoretical studies of RO's for interband transitions have also already been made.⁸⁻¹¹ Although they took into account the effect of many-body interactions in the semiconductor Bloch equations (SBE's) by setting up the pulse frequency with detuning with respect to the unrenormalized energy gap, this frequency was fixed in time and the pulse areas that achieved the best results were not multiples of π . The general plan was to choose simple pulse shapes and vary the area to achieve the deepest RO's subject to this constraint.

Theoretical work in quantum control in semiconductor heterostructures is still a fledgling enterprise, but some relevant research has been done such as in quantum-dot turnstiles,¹² optical bistability all-optical switches in quan-

tum wells (QW's),¹³ optimal control with interband transitions in asymmetric double QW's,¹⁴ and recently Paspalakis *et al.*^{15,16} obtained intersubband population inversions with pulsed THz fields with a time-varying phase in n -type doped QW's. All of them use electromagnetic pulses near resonance as the control. Chirped pulses have been used to some extent in quantum optics. For example, it has been proposed to use linearly chirped ultrafast optical pulses to achieve some degree of state trapping of interband excitation in quantum wells¹¹ in a fashion similar to what has been observed in two-level atomic systems with frequency-modulated pulses.^{17,18}

We here further extend the application of quantum control via chirped pulses in intersubband (ISB) transitions in two-subband quantum wells that was introduced in Ref. 19. There we predicted that substantial RO's can be achieved in ISB transitions of n -type doped QW's provided the center frequency of the terahertz driving pulse self-consistently tracks the time-dependent renormalized ISB gap. The ability to carry out such coherent control at THz frequencies is a potential boon, since both the instantaneous amplitude and phase of the time-dependent polarization can be detected in a straightforward fashion—a task that may be considerably more difficult at optical frequencies. The main novelty of the present work, therefore, is that we show that a pulse whose linear chirp is obtained by a best fit calculated from the fully renormalized transition energy achieves deep Rabi flops, which is a much simpler task than our previous proposal.¹⁹

Furthermore, we also provide results for the polarization of the ISB transitions that were not previously given. The measurement of polarization is also of fundamental importance to quantum control;^{20,21} it is even more important in some cases than the ability to measure the population evolution. This is so because the polarization gives real-time evolution information²² and its measurement is a necessary condition for carrying out quantum computation, while population measurements are typically performed after interaction with external electromagnetic pulses. Results are given for unbiased and dc-biased square QW's. With this study we also fill a gap that was missing in our work, since we have done calculations of quantum control using linear chirp for three-subband QW's,²³ but had not done the same for two-subband systems. Furthermore, the ability to perform quan-

tum control using linear chirp and asymmetric QW's shows that the control scheme is robust.

II. MODEL

Suppose the energy gap of ISB transitions, $\omega(t)=E_1(t)-E_0(t)$, varies with time. How can one find an effective π pulse, i.e., the pulse that maximally inverts the population in this system? We showed in Ref. 19 that one can use a pulse that is suitably chirped (with a time-dependent center frequency) to track self-consistently the renormalized subband splitting in time induced by the pulse itself. The SBE's in GaAs/Al_xGa_{1-x}As QW's can be reduced to effective nonlinear optical Bloch equations (OBE's) because the conduction subbands are approximately parabolic with little mass dispersion, i.e., the dependence on k of the transition energy and the momentum matrix elements is small. This is an aid to the treatment, since models based on the OBE will, to a large extent, be applicable to the ISB transitions. Here we summarize the method proposed in Ref. 19 for achieving RO's in systems with time-dependent energy gaps. Begin with the free-carrier density-matrix equations $\dot{\Delta}=4\mu \text{Im } \sigma F(t)$ and $\dot{\sigma}=i\omega(t)\sigma-i\mu\Delta F(t)$, where Δ is the population difference between upper and lower levels, σ is the off-diagonal element of the density matrix in the basis of the two levels, and μ is the dipole moment. σ is related to the polarization via the dipole moment $\mu(t)=\text{Tr}\{\hat{\sigma}(t)\hat{\mu}\}$. The driving field is chosen to be $F(t)=F_0(t)\exp(-i\int_0^t\omega(s)ds)+\text{c.c.}$. Then, as above, using the transformation $\sigma=\tilde{\sigma}\exp(i\int_0^t\omega(s)ds)$ followed by our rotating-wave approximation (RWA) ansatz, we obtain $\dot{\Delta}=-2i\mu(\tilde{\sigma}-\tilde{\sigma}^*)F_0(t)$ and $\dot{\tilde{\sigma}}=i\mu\Delta F_0(t)$, where without loss of generality we assume the phase dependence of $F_0(t)$ to be constant in time. Integrating the above equations yields

$$\Delta(t)=\Delta_0\cos\left(2\mu\int_0^tF_0(s)ds\right),$$

$$\sigma(t)=\frac{i\Delta_0}{2}\sin\left(2\mu\int_0^tF_0(s)ds\right)\exp\left(i\int_0^t\omega(s)ds\right), \quad (1)$$

where Δ_0 is the equilibrium population difference between the bottom and the upper level. The time-dependent induced polarization is $P(t)=-N\mu\Delta_0\sin[2\mu\int_0^tF_0(s)ds]\sin\int_0^t\omega(s)ds$, which is a simple generalization of the polarization from the usual RO's in two-level systems.⁴ Once again, this discussion shows that the envelope for a $j\pi$ pulse, with its center frequency varying in time, is the same as in the case where the levels are time independent. This will now be applied to RO's in ISB transitions.

The resonant ISB THz response of modulation-doped n -type QW's is known to be highly nonlinear.²⁴ As electrons undergo transitions between the two subbands, the band bending is modified dynamically. Other nonlinearities include time-dependent Pauli blocking and excitation-induced dephasing. The result is that the ISB plasmon exhibits a significant nonlinear response. (By ISB plasmons we mean the long-wavelength electron oscillations as they collectively

perform ISB transitions driven by the THz field polarized perpendicular to the QW plane.) Our approach is to apply the time-dependent Hartree approximation (TDHA) to describe the ISB response to a strong THz field. This has been used in Ref. 25 to describe the experimentally observed nonlinearities in QW's.^{26,27} Li and Ning²⁸ showed that the TDHA with cw THz driving is valid for wide GaAs QW's of 150 Å in width at carrier densities $\approx 10^{12}$ e/cm² since under these QW parameters the depolarization effect was dominant in determining the absorbance line shape and peak position. As the strength of the depolarization effect grows approximately linearly with well width, we expect that in a wider well of 300 Å with a smaller carrier density of 3.0×10^{11} e/cm² the depolarization effect will still be dominant in determining the optical properties of the QW; hence we expect the TDHA to be valid then as well. For pulse durations of several picoseconds, the bandwidth is narrow enough that one can assume the results are close enough to those of cw THz driving. The cases we concentrate on fall well within this range of validity. As such, exchange and exchange-correlation effects are expected to be small for the purposes of this study. Furthermore, for symmetric QW's Olaya-Castro *et al.*²⁹ showed they are not relevant. Once one sums over momenta the exchange terms of the density-matrix equations disappear. We use the foregoing treatment of a two-level system to obtain effective π THz pulses. Having obtained these pulses, we use them in numerical computations based on the TDHA to calculate $\omega(t)$ and thus the THz response of the QW.

The treatment of the nonlinear THz ISB response of QW's is discussed in depth elsewhere.³⁰ Here, we quote the essential results. We have shown that the TDHA can be conveniently restated in terms of the density matrix.³⁰ The density-matrix equations for ISB transitions in an asymmetric QW are

$$\dot{\Delta}=-\gamma_1(\Delta-\Delta_0)+4\text{Im}\sigma V(t),$$

$$\dot{\sigma}=i\omega_{10}\sigma-\gamma_2\sigma-i\Delta V(t)$$

$$-i\sigma\{\alpha[\zeta\text{Re}\sigma+\beta(\Delta-\Delta_0)/4]+F(t)(\mu_{11}-\mu_{00})\}, \quad (2)$$

where $V(t)=\mu_{10}F(t)+\alpha[\text{Re}\sigma-\zeta(\Delta-\Delta_0)/4]$, ω_{10} is the Hartree self-consistent QW ISB energy gap, $\gamma_1=1/T_1$, and $\gamma_2=1/T_2$. The constant coefficients α , β , and ζ are due to Coulomb interactions. They are numerically calculated from the Hartree approximation.³⁰ (They are roughly proportional to N_sL_{QW} , where L_{QW} is the QW width.) In a symmetric QW the effective Bloch equations (2) are further simplified since $\zeta=0$ and $\mu_{00}=\mu_{11}$. Using our RWA ansatz we can recast Eq. (2) in the free-carrier form if we take the pulse center frequency as

$$\omega(t)=\omega_{10}-\alpha\Delta/2-\alpha\beta(\Delta-\Delta_0)/4. \quad (3)$$

But for asymmetric QW's we find numerically that we obtain more accurate control over the populations if we add the asymmetric correction of the energy renormalization given in Eq. (2) to the pulse center frequency. We use

$$\omega(t) = \omega_{10} - \alpha\Delta/2 - \alpha\beta(\Delta - \Delta_0)/4 - \alpha\zeta \text{Re } \sigma. \quad (4)$$

This is likely so because our RWA ansatz starts to break down at lower values of the THz field amplitude in asymmetric QW's as compared with symmetric QW's, due to optical rectification (zero-frequency response which generates a dc polarization) and second-harmonic generation (second-order responses not present in symmetric QW's). With the information that we can recast Eq. (2) into the free-carrier form and obtain Rabi oscillations, we can design π pulses on demand for n -type doped QWs. This approach could in principle be applied to more complex systems, such as to ISB transitions with mass dispersion, exchange interaction, and electron-electron scattering, and to interband transitions; in such cases, we merely utilize the appropriate form of $\omega(t)$. The two-level model should be accurate provided the renormalized energy does not depend too strongly on k .

III. NUMERICAL RESULTS

We now present numerical results of the action of appropriately designed π pulses on n -type modulation-doped QW's. The GaAs/Al_xGa_{1-x}As square QW structure used for our calculations is 300 Å wide and 200 meV deep. We take $T_1=0.66$ ns, $T_2=6.6$ ps ($\gamma_2=0.1$ meV), and the temperature $T=4$ K. In all cases, the pulse envelopes $F_0(t)$ are Gaussian. Equations (2) were integrated using the fourth-order Runge-Kutta method with 2048 steps per cycle of drive. In the results for the unbiased QW that follow the pulse center frequency was given by a linear fit of $\omega(t)$ given by Eq. (3) for the unbiased QW or by Eq. (4) for the biased QW.

The linear fit of $\omega(t)$ given in Eq. (3) is basically the interpolation between the $\omega(\Delta_0)$ given by the initial value of the population difference $\Delta_0=1$ and $\omega(\Delta_f)$ given by the final value of the population difference Δ_f we wish to achieve. This final value is obtained from the results given by the full numerical integration of Eq. (2) with the pulse center frequency given self-consistently by Eq. (3) for the unbiased QW. The time interval t_f-t_i is basically the pulse duration; more precisely it is the interval that will give us the best linear fit of Eq. (3) obtained self-consistently. For the biased QW we just have to replace Eq. (3) by Eq. (4) in the reasoning above.

A. Unbiased quantum well

The QW ISB energy ω_{10} is about 3.5 THz (14.4 meV). The coefficients in Eq. (2) are $\alpha=-0.56$, $\beta=2.87$, $\zeta=0$, $\mu_{00}=\mu_{11}$, the equilibrium population difference $\Delta_0=1$, and the dipole moment $\mu_{10}=61.5$ Å.

In Fig. 1, we show that the usual unchirped π pulses do not work well in inverting the populations once the time-dependent depolarization-shift effects, expressed via the nonlinear terms of $\omega(t)$, become relevant; namely, we employ naive π pulses, as shown in Fig. 1(a). Figures 1(b) and 1(c) show the linearly chirped center frequency and the chirped pulse shape, respectively. Our prescription requires a strongly chirped pulse (the blueshift of the initial frequency is due to depolarization shift, which changes sign when there

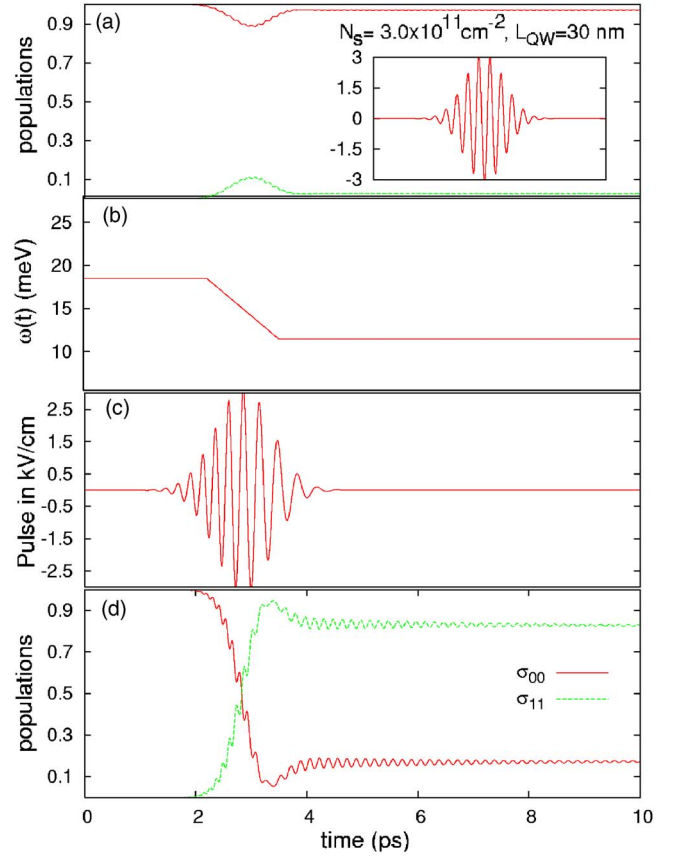


FIG. 1. (Color online) π -pulse-generated RO's of ISB transitions in an unbiased square QW. The density-matrix equations of Eq. (2) are numerically integrated with $\zeta=0$, $\mu_{00}=\mu_{11}$, $\gamma_1=1$ μeV , and $\gamma_2=0.1$ meV. The electron sheet density and QW size are indicated in the figure. The time evolution of the populations driven by pulses without chirp is given in (a), where the inset shows the pulse shape; in (b) we have the center frequency of the pulse, which is given by the linear fit of Eq. (3), in (c) we have the chirped pulse, and in (d) we see that we obtain a fairly deep inversion when the driving pulse is linearly chirped.

is inversion). The chirp in Fig. 1(b) is a linear best fit of the time evolution of $\omega(t)$ in Eq. (3) when its constituent density-matrix elements are given by Eq. (2). We now see whether the inclusion of the time-dependent renormalization of the subband gap within the pulse chirp achieves a higher degree of inversion. In Fig. 4(d) we achieve substantial population inversion after the interaction with the chirped π pulse. The fast small-amplitude oscillations in $\omega(t)$ indicate that our RWA ansatz is not perfect, but as long as these oscillations are relatively small it remains a good approximation. Note that the pulse duration is about one-third of T_2 so that dephasing here does not place a large limitation on the greatest inversion that can be obtained.

The pulses employed above have peak fields of 3 kV/cm. Such large-amplitude pulses are difficult to obtain; however, smaller peak fields imply longer pulse duration for a given value of \mathcal{A} . Chirped pulses with these amplitudes are likely to be obtainable using optical rectification of ultrafast optical pulses in suitably designed nonperiodically poled lithium niobate,³¹ i.e., with linearly growing domain sizes. In Fig. 2

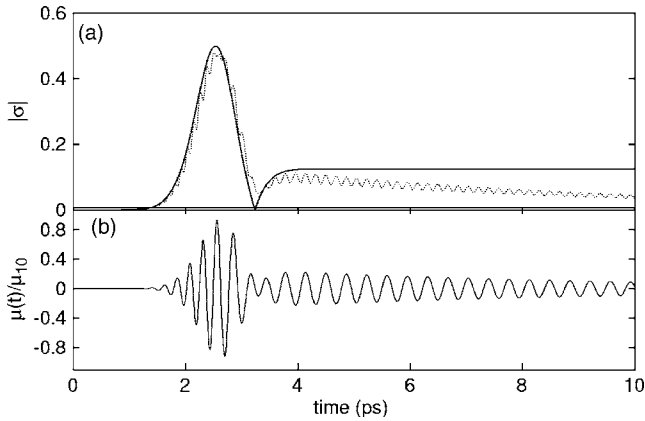


FIG. 2. Polarization data obtained for the square QW driven by a linearly chirped pulse. In (a) we show that our model fits very well the amplitude of the off-diagonal density-matrix element $\sigma(t)$. The solid line is obtained from integration of the free-carrier two-level density-matrix equation, as shown in Eq. (1). The dotted line is obtained from integration of Eq. (2) with the center frequency of the driving pulse given by a linear fit of Eq. (3). The kink in the solid line is due the pulse area being just over π . In (b) we plot the polarization [$\mu(t)=\text{Tr}\{\hat{\sigma}(t)\hat{\mu}\}$] in units of the dipole moment $\mu_{10}=61.5 \text{ \AA}$.

we show that we can track the polarization of the ISB transitions. In Fig. 2(a) we have a fit of the amplitude of $\sigma(t)$ provided by the solution of Eq. (2) by the analytically predicted result given in Eq. (1). The kink in the smooth curve occurs because the pulse area is slightly over π . Since in the original Rabi solution given by Eq. (1) the state of the two-level system can be taken anywhere on the Bloch sphere, that implies we could also take the state of the two-subband QW system anywhere we want; therefore, that implies we have controllability. The phase could also be tracked by our model, but since it is changing quickly in time it would be hard to see the accuracy of the fitting. In Fig. 2(b) we plot the polarization.

B. Biased quantum well

The QW ISB energy ω_{10} is about 3.7 THz (15.1 meV). The coefficients in Eq. (2) are $\alpha=-0.74$, $\beta=6.65$, $\Delta_0=0.94$, $\zeta=-0.61$, $\mu_{10}=58.8 \text{ \AA}$, and the dc bias is 6.7 kV/cm. We again find that unchirped π pulses are ineffective in generating population inversions and no carrier excitation is observed. To achieve inversions now we use a linear fit of the self-consistent gap $\omega(t)$ as given in Eq. (4) for the pulse center frequency. This linear fit is shown in Fig. 3(a) and the pulse shape shown in Fig. 3(b). Due to the asymmetric term and the larger value of the coefficient β , as compared with values for the unbiased QW, the numerical results deviate further from what our RWA ansatz predicts (since we do not obtain a slowly varying rotating frame on the Bloch sphere), but we nevertheless obtain deep inversions as shown in Fig. 3(c). We again emphasize that our RWA ansatz is only used as a guide to find the optimal linear chirp. These results were obtained with five subbands included in the density-matrix equations. As one can see from the near-zero excitation of

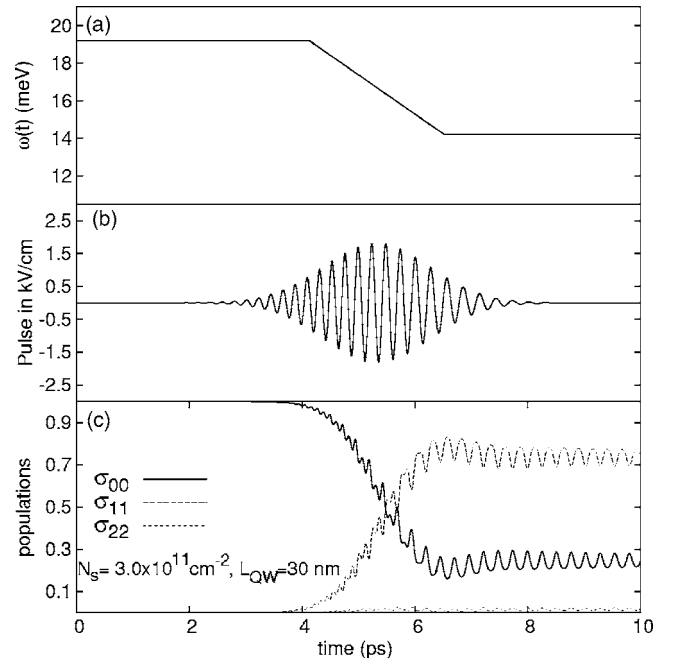


FIG. 3. π -pulse-generated Rabi flops of intersubband transitions in the model of Eq. (2) with $\gamma_1=1 \text{ \mu eV}$ and $\gamma_2=0.1 \text{ meV}$ for a dc-biased square QW with a dc field of 6.7 kV/cm. Five subbands were included in this computation in order to verify the applicability of the two-subband model. The electron sheet density and well size are indicated in the figure. The results are obtained from numerical integration of Eq. (2). In (a) we have the center frequency of the pulse which is given by a linear fit of Eq. (4), in (b) we have the chirped pulse, and in (c) we see that we obtain a fairly deep inversion when the driving pulse is linearly chirped.

the third and higher subbands, the two-subband model is a good approximation. The linear fit of the center frequency as can be seen in Fig. 3 is possibly achievable in the laboratory and similarly provides almost as deep population inversion as in the self-consistent tracking of the gap (not shown here).

In Fig. 4 we show the polarization of the ISB transitions for a dc-biased QW. In Fig. 4(a) we have a fit of the amplitude of $\sigma(t)$ provided by the solution of Eq. (2) by the analytically predicted result given in Eq. (1). Here our ability to track the polarization is smaller than in the unbiased case, because the numerical results deviate further from our RWA ansatz predictions than in the unbiased case; this is mainly due to optical rectification and second-harmonic generation as just described. In Fig. 4(b) we plot the polarization.

IV. CONCLUSION

We have demonstrated theoretically the application of linearly chirped pulses to generate RO's of ISB transitions when the ISB gap varies slowly with time. In a previous paper¹⁹ we considered the case in which the ISB splitting and the pulse center frequency depend self-consistently on the optical pulse. We here demonstrate that effective π pulses that are linearly chirped (a best fit of the self-consistent chirp) can lead to substantial population inversions in symmetric and asymmetric (dc-biased) n -type QW's. By doing

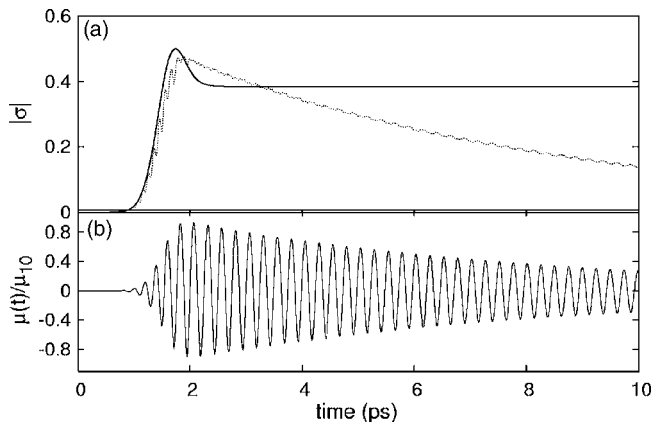


FIG. 4. Polarization data obtained for the biased QW driven by a linearly chirped pulse. In (a) we show that our model still fits the amplitude of off-diagonal density-matrix element $\sigma(t)$ which varies adiabatically. The solid line is obtained from integration of the free-carrier two-level density-matrix equation, as shown in Eq. (1). The dotted line is obtained from integration of Eq. (2) with the center frequency of the driving pulse given by a linear fit of Eq. (3). The pulse area is about 0.7π . In (b) we plot the polarization in units of the dipole moment $\mu_{10}=58.8 \text{ \AA}$.

so, we show that our control mechanism is robust since the chirp does not need to follow exactly the self-consistent solution. Furthermore, we show that not only the populations but also the polarization can be controlled. Moreover, the QW need not be symmetric, which is an advantage to the experimentalist since by applying a dc bias the ISB transition can be tuned into resonance. We find that deep RO's can be achieved even in the presence of realistic values of dephasing for moderate doping with peak fields on the order of 1.5 kV/cm. More broadly, the technique may be helpful in generating RO's in other systems exhibiting time-dependent level renormalizations, and may find application in coherent control and quantum information processing.^{21,20} Recently,³² phase-resolved experiments on ISB RO's in QW's in the tens of THz have been carried out; in principle, the method proposed here can be applied to this frequency range of ISB transitions as well.

ACKNOWLEDGMENTS

A.A.B. would like to thank H. N. Nazareno for useful discussions. D.S.C. acknowledges the support of the National Science Foundation Grant No. ECS 0523923.

¹I. I. Rabi, Phys. Rev. **51**, 652 (1937).
²S. L. McCall and E. L. Hahn, Phys. Rev. **183**, 457 (1968).
³L. Allen and J. H. Eberly, *Optical Resonance and Two-Level Atoms* (Dover, New York, 1987).
⁴V. M. Akulin and N. V. Karlov, *Intense Resonant Interactions in Quantum Electronics* (Springer-Verlag, Berlin, 1992).
⁵S. T. Cundiff, A. Knorr, J. Feldmann, S. W. Koch, E. O. Gobel, and H. Nickel, Phys. Rev. Lett. **73**, 1178 (1994).
⁶A. Schulzgen, R. Binder, M. E. Donovan, M. Lindberg, K. Wundke, H. M. Gibbs, G. Khitrova, and N. Peyghambarian, Phys. Rev. Lett. **82**, 2346 (1999).
⁷A. Zrenner, E. Beham, S. Stuffer, F. Findeis, M. Bichler, and G. Abstreiter, Nature (London) **418**, 612 (2002).
⁸R. Binder, S. W. Koch, M. Lindberg, N. Peyghambarian, and W. Schafer, Phys. Rev. Lett. **65**, 899 (1990).
⁹T. Ostreich and A. Knorr, Phys. Rev. B **48**, 17811 (1993).
¹⁰A. Knorr, Th. Ostreich, K. Schonhammer, R. Binder, and S. W. Koch, Phys. Rev. B **49**, 14024 (1994).
¹¹S. Hughes, W. Harshawardhan, and D. S. Citrin, Phys. Rev. B **60**, 15523 (1999).
¹²P. I. Tamborenea and H. Metiu, Phys. Rev. Lett. **83**, 3912 (1999).
¹³H. O. Wijewardane and C. A. Ullrich, Appl. Phys. Lett. **84**, 3984 (2004).
¹⁴J. L. Krause, D. H. Reitze, G. D. Sanders, A. V. Kuznetsov, and C. J. Stanton, Phys. Rev. B **57**, 9024 (1998).
¹⁵E. Paspalakis, M. Tsaousidou, and A. F. Terzis, Phys. Rev. B **73**, 125344 (2006).
¹⁶E. Paspalakis, M. Tsaousidou, and A. F. Terzis, J. Appl. Phys. **100**, 044312 (2006).
¹⁷G. S. Agarwal and W. Harshawardhan, Phys. Rev. A **50**, R4465 (1994).
¹⁸M. W. Noel, W. M. Griffith, and T. F. Gallagher, Phys. Rev. A **58**, 2265 (1998).
¹⁹A. A. Batista and D. S. Citrin, Phys. Rev. Lett. **92**, 127404 (2004).
²⁰M. S. Sherwin, A. Imamoglu, and T. Montroy, Phys. Rev. A **60**, 3508 (1999).
²¹B. E. Cole, J. B. Williams, B. T. King, M. S. Sherwin, and C. R. Stanley, Nature (London) **410**, 60 (2001).
²²C. W. Luo, K. Reimann, M. Woerner, T. Elsaesser, R. Hey, and K. H. Ploog, Phys. Rev. Lett. **92**, 047402 (2004).
²³A. A. Batista, Phys. Rev. B **73**, 075305 (2006).
²⁴M. S. Sherwin, K. Craig, B. Galdrikian, J. N. Heyman, A. Markelz, K. Campman, S. Fafard, P. F. Hopkins, and A. C. Gossard, Physica D **83**, 229 (1995).
²⁵M. Zaluźny, J. Appl. Phys. **74**, 4716 (1993).
²⁶J. N. Heyman, K. Craig, B. Galdrikian, M. S. Sherwin, K. Campman, P. F. Hopkins, S. Fafard, and A. C. Gossard, Phys. Rev. Lett. **72**, 2183 (1994).
²⁷J. N. Heyman, K. Unterrainer, K. Craig, B. Galdrikian, M. S. Sherwin, K. Campman, P. F. Hopkins, and A. C. Gossard, Phys. Rev. Lett. **74**, 2682 (1995).
²⁸J. Li and C. Z. Ning, Phys. Rev. Lett. **91**, 097401 (2003).
²⁹A. Olaya-Castro, M. Korkusinski, P. Hawrylak, and M. Y. Ivanov, Phys. Rev. B **68**, 155305 (2003).
³⁰A. A. Batista, P. I. Tamborenea, B. Birnir, M. S. Sherwin, and D. S. Citrin, Phys. Rev. B **66**, 195325 (2002).
³¹Y.-S. Lee, T. Meade, V. Perlin, H. Winful, T. B. Norris, and A. Galvanauskas, Appl. Phys. Lett. **76**, 2505 (2000).
³²C. W. Luo, K. Reimann, M. Woerner, T. Elsaesser, R. Hey, and K. H. Ploog, Semicond. Sci. Technol. **19**, S285 (2004).